



Full Length Article

Prediction method for ignition delay time of liquid spray combustion in constant volume chamber

Jiun Cai Ong^{a,*}, Kar Mun Pang^b, Jens Honore Walther^{a,c}

^a Department of Mechanical Engineering, Technical University of Denmark, Nils Koppels Allé, 2800 Kgs. Lyngby, Denmark

^b MAN Energy Solutions, Tegholmsgade 41, 2450 København SV, Denmark

^c Computational Science and Engineering Laboratory, ETH Zürich, Clausiusstrasse 33, Zürich CH-8092, Switzerland



ARTICLE INFO

Keywords:

Ignition delay time
Homogeneous reactor
Probability density function
Large eddy simulations
n-Dodecane spray

ABSTRACT

A prediction method, known as the Coupled Time Scale (CTS) method, is proposed in the current work to estimate the ignition delay time (IDT) of liquid spray combustion by only performing an inert spray simulation and a zero-dimensional (0-D) homogeneous reactor (HR) simulation. The method is built upon the assumption that if the majority of the vapor regions in a spray has a composition close to the most reactive mixture fraction, which can be obtained by performing 0-D HR calculations, these regions will then have a high probability to undergo high-temperature ignition in the spray. The proposed method is applied to estimate the high-temperature IDT of n-dodecane sprays. Two nozzle diameters (D_{noz}) of 90 μm and 186 μm which correspond to Spray A and Spray D in the Engine Combustion Network [1] respectively, are considered. Both D_{noz} are tested at three ambient temperatures (T_{am}) of 800 K, 900 K, and 1000 K. The fidelity of the proposed CTS method is verified by comparing the predicted IDT against CFD simulated IDT and measured IDT. Comparison of the estimated IDT from the CTS method to the measured IDT yields a maximum relative difference of 24%. Meanwhile, a maximum relative difference of 33% is found between the IDTs computed from the CTS method and the large eddy simulations of the associated reacting sprays across the different T_{am} , D_{noz} , and chemical mechanisms considered in this study.

1. Introduction

Ignition delay time (IDT) plays a vital role in a diesel engine as it influences the engine combustion and emission characteristics. Hence, an accurate prediction of the IDT in numerical studies is of the utmost importance. Apart from the mixing process, the type of chemical mechanisms used in numerical studies have significant influence on the prediction of IDT. A detailed chemical mechanism consisting of hundreds of species is expected to provide a better accuracy across a wide range of conditions, but the use of such a large mechanism is computationally demanding. This leads to the popularity of implementing reduced mechanisms which retain only the essential chemical species and reactions for specific conditions to achieve a balance between accuracy and computational cost. Nevertheless, any chemical mechanisms must first be validated in zero-dimensional (0-D) homogeneous stagnant adiabatic mixtures, such as shock tubes [2] and rapid compression machines [3], before they are used for applications in three-dimensional (3-D) computational fluid dynamics (CFD). Using the correlation

between temperature and mixture fraction predicted from CFD simulations [4,5], the most reactive mixture fraction (Z_{mr}) and the associated IDT (IDT_{mr}) [6] can be calculated from 0-D homogeneous reactor (HR) simulations of a diesel spray flame. The parameter Z_{mr} , defined as the mixture fraction which has the shortest IDT, is known to play an important role in the autoignition process [7]. Autoignition in pure gaseous cases have shown to occur where the mixture composition is close to Z_{mr} and has low scalar dissipation rates [7]. Numerous studies in spray autoignition [8–10] showed similar observations in the ignition process. There are, however, also numerical studies [11–13] which disagreed with this observation and showed the ignition to occur in mixtures richer than Z_{mr} . On the other hand, the corresponding IDT_{mr} , which is also computed from 0-D HR simulations, is unable to represent the IDT of spray combustion as turbulence effects of fluid flow and the liquid spray characteristics (e.g. breakup and evaporation) are not considered [6] in 0-D HR simulations. This finding is supported by Dahms et al. [14] who carried out one-dimensional flamelet calculations at the standard Spray A condition from the Engine Combustion Network

* Corresponding author.

E-mail address: jcong@mek.dtu.dk (J.C. Ong).

<https://doi.org/10.1016/j.fuel.2020.119539>

Received 24 July 2020; Received in revised form 3 October 2020; Accepted 15 October 2020

Available online 4 December 2020

0016-2361/© 2020 Elsevier Ltd. All rights reserved.

(ECN) [1]. It is thus apparent that performing a full reacting spray simulation, which accounts for the turbulent flow field, is essential to obtain the IDT of the spray combustion. However, this process may be costly, depending on the size of the chemical mechanism, grid resolutions, and combustion models used.

Setting against this background, the present work first examines the mixture fraction of the ignition mixture, then proposes a method to estimate the IDT of spray combustion by only computing the inert spray and by performing 0-D HR calculations, without the need to perform a full reacting spray simulation. The method assumes that if the majority of the spray regions has a composition close to Z_{mr} , then the regions will have a high probability to undergo high-temperature ignition. The method requires the probability density function (PDF) of the mixture fraction (Z) computed from 3-D simulations of inert sprays, as well as the Z_{mr} and IDT_{mr} obtained from 0-D HR simulations. Since the proposed approach is based on the mixing time scale from inert spray simulations and chemical time scale from 0-D HR simulations, it is henceforth known as the Coupled Time Scale (CTS) method.

The paper is structured as follows. The next section describes the experimental data used for model validation as well as the numerical setup. This is followed by the results from inert spray simulations, 0-D HR simulations, and reacting spray simulations in Sections 3.1, 3.2, and 3.3, respectively. The proposed CTS method is subsequently described in Section 3.4. Verification of the estimated IDT against measured and CFD simulated IDT is also shown in this section. Next, a sensitivity study of the proposed CTS method using different mechanisms is carried out and shown in Section 3.7. Conclusions from this work are outlined in the final section.

2. Case descriptions & CFD model formulation

The simulated spray combustion cases conducted in the present study correspond to the Spray A [1] and Spray D conditions [1,15] of the ECN. Details of the ambient gas composition, thermodynamic conditions, and injector parameters are shown in Table 1. The nominal nozzle diameter (D_{noz}) for Spray A and Spray D are 90 μm and 186 μm , respectively. Both Spray A and Spray D involve injecting liquid *n*-dodecane ($\text{C}_{12}\text{H}_{26}$) through their respective nozzle with an injection pressure of 150 MPa into a constant volume combustion vessel. Three ambient temperatures (T_{am}) of 800 K, 900 K, and 1000 K are tested in the present study. In the inert spray case, the molar fraction of O_2 is set to 0%, whereas in the reacting spray case, it is set to 15%. An Eulerian-Lagrangian approach is used within the LES framework for the spray modeling in OpenFOAM-v1712. Both temporal and spatial terms are discretized using second-order schemes. The sub-grid scale (SGS) is modeled using the Dynamic k -equation [16]. The injected liquid phase of $\text{C}_{12}\text{H}_{26}$ is modeled as discrete parcels whose motion is described using the Lagrangian particle tracking approach. Spray breakup is modeled by the Reitz-Diwakar spray model [17], where the stripping breakup constant, C_s is set to 10. The skeletal $\text{C}_{12}\text{H}_{26}$ mechanism developed by Yao

Table 1
Injector specifications and operating conditions [1,15].

	Spray A	Spray D
Nozzle diameter, D_{noz} [μm]	90	186
Injected fuel mass flow rate [g/s]	2.295	11.71
Injection pressure [MPa]	150	
Ambient density, ρ_{am} [kg/m^3]	22.8	
Ambient temperature, T_{am} [K]	800, 900, 1000	
Ambient gas composition [mol %]	Inert	Reacting
O_2	0.00	15.00
N_2	89.71	75.15
CO_2	6.52	6.22
H_2O	3.77	3.62

et al. [18] (54 species and 269 reactions) is used in this work. Detailed description of the mechanism can be found therein [18]. The mechanism has shown good performance in spray combustion context [19,20]. The partially stirred reactor (PaSR) [21] combustion model, coupled with Chemistry Coordinate Mapping (CCM) [22], is used here to account for the turbulence-chemistry interaction. The mixing constant, C_{mix} in the PaSR model is set to 0.3. Details about the CCM approach is available in [22,23]. The computational domain is a constant volume cubic chamber with side lengths of 108 mm, which corresponds to the dimension of the experimental combustion vessel [1]. The ambient mixture composition, pressure, and temperature are initiated as uniform fields based on the values shown in Table 1, while the velocity field is set to zero. All boundaries are set as no-slip wall with Neumann boundary condition for the ambient mixture composition, pressure, and temperature. The injector is placed at the center of one of the chamber walls. A uniform mesh spacing of 0.125 mm is used for the spray combustion region (80 mm axially and 15 mm radially from the nozzle location) with coarser mesh outside the region.

3. Results & discussion

3.1. Inert spray

The validation of the computational setup is carried out by comparing the liquid penetration length (LPL) and vapor penetration length (VPL) with experimental data [1,15,24]. LPL is defined as the maximum axial location from the injector to the location where 95% of the total liquid mass is found. VPL is determined using the farthest downstream location of 0.1% fuel mass fraction. It is shown in Fig. 1 that the simulated LPL and VPL for Spray A and Spray D agree well with measurement data. The LPLs are shown to decrease with increasing T_{am} for both Spray A and Spray D, with the trend being more apparent in the Spray D cases [24]. On the other hand, the VPLs for Spray A and Spray D are shown to be insensitive to temperature variation. This also agrees with the experimental findings [24].

From the inert spray simulations, one can extract the temperature (T) in the flow field as a function of the local mixture fraction (Z) for Spray A and Spray D at various T_{am} . The upper boundary of the T - Z diagram follows a quadratic relation,

$$T(T_{am}, Z) = T_{am} + b(T_{am})Z + c(T_{am})Z^2, \quad 800\text{K} \geq T_{am} \geq 1000\text{K} \quad (1)$$

where $b(T_{am}) = -4T_{am} + 2700$, and $c(T_{am}) = 6T_{am} - 4700$ for Spray A; $b(T_{am}) = -2T_{am} + 1100$, and $c(T_{am}) = T_{am} - 300$ for Spray D. This fitting function is known as the spray mixing line, which shows the maximum T that can be achieved at different Z for the inert spray case. The T - Z diagram and the corresponding spray mixing line for Spray A at $T_{am} = 900$ K is provided in Fig. 2 for illustration purpose. The most

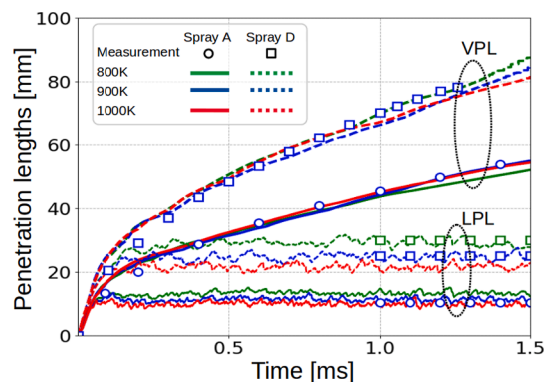


Fig. 1. Temporal evolution of liquid penetration lengths (LPL) and vapor penetration lengths (VPL) for Spray A and Spray D at varying T_{am} . Symbols represent measurement data.

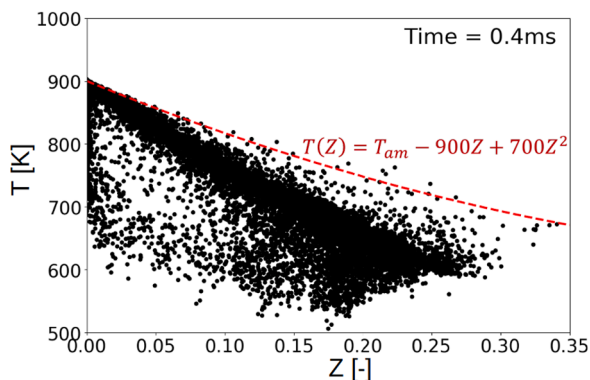


Fig. 2. Scatter plots of temperature (T) and mixture fraction (Z) for Spray A at T_{am} of 900 K. Spray mixing line is represented by the red dashed-line.

reactive state, Z_{mr} and IDT_{mr} is obtained by performing 0-D HR simulations along the spray mixing line, which is shown in the next section.

3.2. Autoignition of homogeneous mixture

The 0-D HR simulations are carried out using the ANSYS CHEMKIN-PRO software. The predicted IDT profiles for Spray A and Spray D from the 0-D HR simulation using the Yao mechanism are shown in Fig. 3. The IDT here is defined as the time when the mixture temperature increases to 400 K above the initial temperature ($T_{t=0}$). From the figure, one can extract Z_{mr} which is characterized as the Z with the shortest IDT, also known as IDT_{mr} , for different T_{am} . It is depicted in Fig. 3 that Z_{mr} increases with increasing T_{am} for both Spray A and Spray D.

The extracted IDT_{mr} for Spray A and Spray D are shown together with the measured IDT from reacting spray experiments in Fig. 4. It is apparent from the figure that IDT_{mr} are significantly lower than the measured reacting spray IDT. Furthermore, the difference in IDT_{mr} between Spray A and Spray D does not vary with T_{am} . This observation is inconsistent with the experimental findings [15,25] which shows increasing difference in the IDT between Spray A and Spray D as T_{am} decreases. This result also indicates that IDT_{mr} itself is unable to represent the IDT of the reacting spray.

3.3. Reacting spray

In this section, 3-D LES of reacting spray cases are performed using the same setup used in Section 3.1. The reacting spray cases are validated by comparing the simulated IDTs for Spray A and Spray D at different T_{am} against measurement data, which is depicted in Fig. 4. The computed IDT from 3-D LES (henceforth known as $IDT_{HT,CFD}$) have the

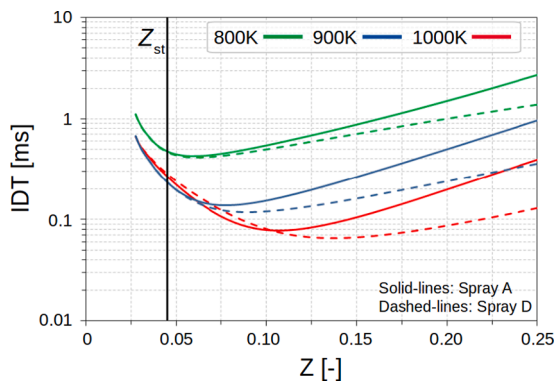


Fig. 3. Ignition delay time (IDT) of homogeneous mixtures as a function of mixture fraction (Z) for Spray A and Spray D at different T_{am} . Solid black line represents stoichiometric mixture fraction, $Z_{st} = 0.045$.

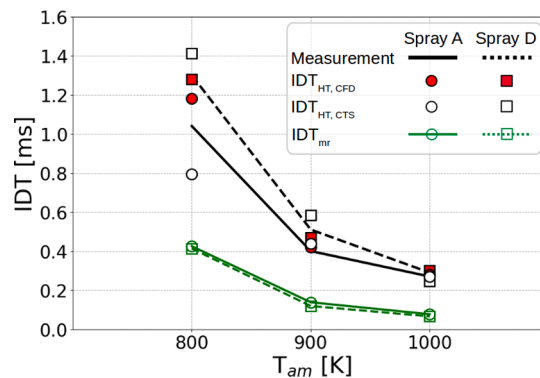


Fig. 4. Comparison of most reactive IDT (IDT_{mr}), IDT from the CTS method ($IDT_{HT,CTS}$), IDT from CFD simulations ($IDT_{HT,CFD}$), and measurements for Spray A and Spray D at various T_{am} .

same definition as the measurement data, which is the time from start of injection to the time when the maximum rate of maximum temperature rise in the domain occurs [13]. This definition is in accordance with the ECN recommendation [1]. The predicted $IDT_{HT,CFD}$ across different T_{am} and D_{noz} has a maximum relative difference of 14% compared to measurements.

Further analysis of the ignition process in mixture fraction space for Spray A and Spray D at different T_{am} is conducted by examining the transition from low- to high-temperature ignition events, as shown in Fig. 5. The low-temperature ignition first initiates in the fuel-lean region ($Z < Z_{st}$) (not shown here), where Z_{st} is the stoichiometric mixture fraction with a value of 0.045. It is followed by an apparent temperature rise within the fuel-rich region ($Z > Z_{st}$), as shown in Fig. 5a. Thereafter, the temperature rise “propagates” towards a relatively less-rich mixture where the high-temperature ignition occurs, which is illustrated in Fig. 5c. These observations agree with the findings from the LES performed by Pei et al. [13]. It is notable in Fig. 5b that the transition from the low- to high-temperature ignition stage is shown to occur near Z_{mr} . This implies that Z_{mr} plays an important role in the ignition process.

3.4. Coupled Time Scale (CTS) method

Recently, Borghesi et al. [9] investigated the spontaneous ignition of n -heptane sprays at high-pressure using 3-D direct numerical simulations. The study demonstrated that the higher the probability of having regions with composition closer to Z_{mr} , the larger the number of ignition spots. This leads to the proposed CTS method which builds upon similar hypothesis that, if the majority of the vapor regions in a spray has composition close to the Z_{mr} , these regions will undergo high-temperature ignition and ultimately result in the ignition of the whole spray. Two main assumptions are considered: i) the mixture composition at Z_{mr} undergoing the high-temperature ignition has an IDT equal to IDT_{mr} , and ii) the whole spray is assumed to undergo the high-temperature ignition when the majority of the vapor regions in the spray has a mixture composition equal to Z_{mr} . It is also worth mentioning that the scalar dissipation rate is not considered in the proposed method. In order to examine the distribution of mixture composition in the spray, a PDF of Z is computed. It is expected that the spray distribution in the reacting spray case (before ignition) and in the inert spray case are similar to one another. Therefore, the PDF of Z is carried out only for the inert spray cases.

3.5. Probability density function of Z for inert sprays

The PDF of Z is computed from the inert spray cases in Section 3.1 to examine the distribution of the mass originated from the fuel. The PDF of Z is defined as

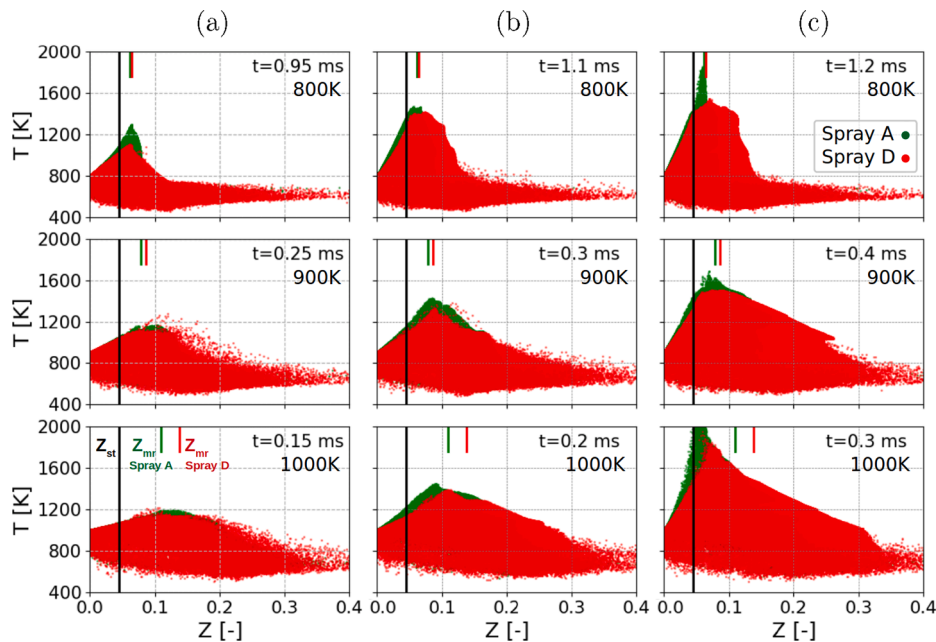


Fig. 5. Temporal evolution of the scatter plot of temperature (T) and mixture fraction (Z) for Spray A and Spray D at various T_{am} conditions. Solid vertical black line represents the stoichiometric mixture fraction (Z_{st}). Green and red solid vertical lines represent most reactive mixture fraction (Z_{mr}) for Spray A and Spray D, respectively. Columns (a), (b), and (c) represent the low-temperature ignition stage, transition stage, and high-temperature ignition stage, respectively.

$$p(Z) = \frac{\sum_{i=1}^{N_{cell}} \rho_i Z_i V_i \alpha_i}{\Delta Z \sum_{i=1}^{N_{cell}} \rho_i Z_i V_i}, \quad \alpha_i = \begin{cases} 1, & Z_i \in (Z - \Delta Z/2, Z + \Delta Z/2) \\ 0, & \text{otherwise} \end{cases} \quad (2)$$

where V_i is the volume of the i -th mesh cell, ρ_i is the density, and N_{cell} is the total number of cells in the domain. ΔZ is the interval of Z and is set to 0.005. A moving average is then carried out on the $p(Z)$ to filter out fluctuations. Fig. 6 illustrates the different time instances of $p(Z)$ obtained from the inert Spray A case at $T_{am} = 900$ K. The Z value with the highest probability is denoted as Z_{peak} , which is indicated by the symbols in Fig. 6. It is noticeable from the figure that the Z_{peak} at $t = 0.1$ ms and 0.2 ms are debatable as the PDF of Z at these two time instances shows a plateau with two peaks. Nevertheless, it does not change the fact that Z_{peak} is still decreasing over time as the PDF of Z is shifting towards Z_{st} .

The Z_{peak} at each time instance are extracted and subsequently plotted in Figs. 7a and 7b for Spray A and Spray D, respectively, at different T_{am} . It is shown in Fig. 7 that in all three T_{am} cases the Z_{peak} are initially fuel rich ($Z > 0.1$) and slowly decreasing towards Z_{st} as time

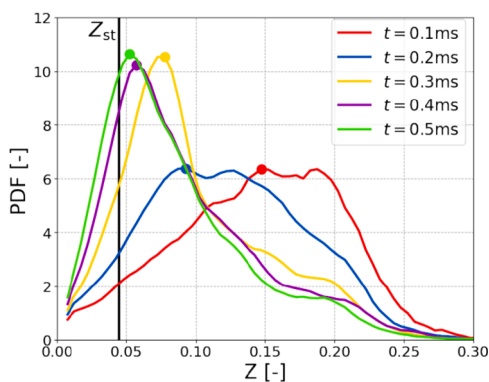


Fig. 6. Probability density function (PDF) of mixture fraction (Z) at different time instances for Spray A at $T_{am} = 900$ K. Solid black line represents stoichiometric mixture fraction (Z_{st}). Symbols represent mixture fraction at peak PDF (Z_{peak}).

progresses. This is expected as more liquid fuel evaporates and mixes with the ambient air. It is also notable that the initial Z_{peak} in Spray A is relatively richer than in Spray D (cf. Figs. 7a and 7b). However, the rate at which Z_{peak} approaches Z_{st} is much faster in Spray A than in Spray D. This implies that Spray A has a faster mixing time than in Spray D, which is similarly shown in [25,26]. As the mixing time is slower in Spray D, the majority of the spray is more fuel-rich than in Spray A at the same time instances, as shown in Fig. 7.

3.6. IDT from CTS method

The Z_{mr} obtained from the 0-D HR simulation in Section 3.2 at various T_{am} are represented by horizontal dashed-lines in Fig. 7. The time instance when Z_{peak} intersects with the horizontal Z_{mr} line is denoted as t_{mr} , which is represented as symbols in Fig. 7. The parameter t_{mr} indicates the time taken for the majority of the spray to achieve a mixture composition close to Z_{mr} . It can also be interpreted as the mixing time of the spray to attain a mixture composition which is favorable for the high-temperature ignition. Following the assumption (ii) highlighted in Section 3.4, once t_{mr} is attained the spray undergoes a similar autoignition process as computed in the 0-D HR simulations with an IDT of IDT_{mr} . Therefore, the high-temperature IDT of spray combustion can be estimated by summing up t_{mr} and its corresponding IDT_{mr} . This estimated high-temperature IDT from using the CTS method is henceforth known $IDT_{HT,CTS}$.

The $IDT_{HT,CTS}$ for each case is shown in Fig. 4, together with the measured IDT [1,15] and CFD simulated $IDT_{HT,CFD}$. A comparison of $IDT_{HT,CTS}$ with the measurement data shows a good agreement with the relative differences being less than 24%. Furthermore, the comparison of $IDT_{HT,CTS}$ with $IDT_{HT,CFD}$ also shows good agreement for both Spray A and Spray D cases across all three T_{am} . The relative differences of $IDT_{HT,CTS}$ to $IDT_{HT,CFD}$ are less than 33% across different T_{am} and D_{noz} . Scalar dissipation rate is shown to play a significant role at low T_{am} [27]. Its absence from the proposed method is likely the reason for the larger discrepancy observed at T_{am} of 800 K (cf. Fig. 4).

It is shown experimentally in [15,25] that IDT for Spray D is relatively longer than Spray A. In addition, the difference between measured IDTs for Spray A and Spray D increases as T_{am} decreases. It is previously

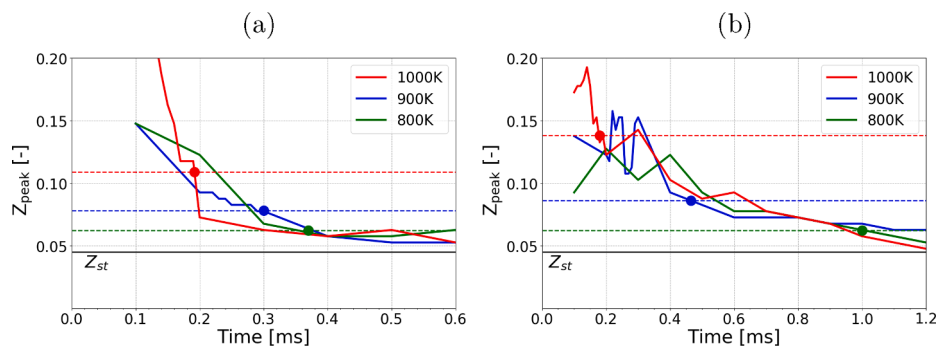


Fig. 7. Temporal evolution of mixture fraction at peak PDF (Z_{peak}) for (a) Spray A and (b) Spray D at different T_{amb} . Horizontal dashed-lines represent most reactive mixture fraction (Z_{mr}) at different T_{amb} . Symbols (●) indicate t_{mr} .

shown in Section 3.2 that IDT_{mr} fails to capture these experimental trend. In contrast, $\text{IDT}_{\text{HT,CTS}}$ is depicted in Fig. 4 to correspond well with the measurement trend observed across different T_{amb} and D_{noz} . There is, however, a discrepancy at T_{amb} of 1000 K where $\text{IDT}_{\text{HT,CTS}}$ for Spray D is shorter than Spray A. This can be attributed to the relative difference of the measured IDT between Spray A and Spray D at 1000 K ($\sim 0.02\text{ms}$) being within the uncertainty of the CTS method. Nevertheless, it is evident that between IDT_{mr} and $\text{IDT}_{\text{HT,CTS}}$, the latter has a better agreement with the experimental trend.

Another important feature of the proposed CTS method is the ability to quantify the spray mixing time needed to achieve favorable mixture composition for high-temperature ignition through the parameter t_{mr} . This can be demonstrated by analyzing the IDTs for the Spray A and Spray D cases at T_{amb} of 800 K. It is previously shown in Fig. 3 that the most reactive states (Z_{mr} and IDT_{mr}) at 800 K are similar for both Spray A and Spray D. However, a noticeable difference in the $\text{IDT}_{\text{HT,CTS}}$ for Spray A and Spray D at T_{amb} of 800 K can be seen in Fig. 4. This result can be attributed to the relatively longer t_{mr} obtained for Spray D than Spray A at 800 K (cf. Fig. 7). This implies that more time is needed to achieve the optimum composition for ignition in Spray D than in Spray A due to the former having a slower mixing time, which is similarly postulated in [24,25]. Overall, the results have demonstrated the feasibility of the proposed CTS method in estimating the IDT for reacting spray combustion without the need to perform a full reacting spray combustion simulation, as well as highlight the advantages of $\text{IDT}_{\text{HT,CTS}}$ over IDT_{mr} . The IDTs calculated using the three methods across different conditions are also tabulated in Table 2 to facilitate quantitative comparisons.

3.7. Sensitivity of chemical mechanism

In this section, the sensitivity of the proposed CTS method to the chemical mechanisms used is evaluated by testing three other reduced mechanisms: (1) the 57-species mechanism by Cai et al. [28] (Cai), (2) the 130-species mechanism by Ranzi et al. [29] (Polimi), and (3) the 257-species mechanism by Narayanaswamy et al. [30] (Stanford). Detailed description of each mechanisms can be referred to in their original publications. The same methodology as those carried out for the Yao mechanism in the previous sections is applied to the three aforementioned mechanisms. It is worth mentioning that the sensitivity study

Table 2
Summary of IDTs for Spray A and Spray D at various T_{amb} .

	Exp [ms]	IDT_{mr} [ms]	$\text{IDT}_{\text{HT,CFD}}$ [ms]	$\text{IDT}_{\text{HT,CTS}}$ [ms]
Spray A, 800 K	1.04	0.43	1.18	0.80
Spray A, 900 K	0.40	0.14	0.42	0.44
Spray A, 1000 K	0.27	0.08	0.28	0.27
Spray D, 800 K	1.30	0.41	1.28	1.41
Spray D, 900 K	0.51	0.12	0.47	0.58
Spray D, 1000 K	0.29	0.07	0.30	0.25

is only carried out for Spray A at T_{amb} of 900 K.

The IDTs profiles along the spray mixing line from all three chemical mechanisms are computed from the 0-D HR simulations and shown in Figs. 8. The Z_{mr} obtained from Fig. 8 for each chemical mechanism is plotted in Fig. 9. Their corresponding t_{mr} are then extracted from the intersection points between Z_{peak} and Z_{mr} . Table 3 shows the calculated $\text{IDT}_{\text{HT,CTS}}$ for each mechanism. It is also shown that the relative difference between $\text{IDT}_{\text{HT,CTS}}$ and $\text{IDT}_{\text{HT,CFD}}$ for the Cai mechanism is only 5.1%. It is important to note that the $\text{IDT}_{\text{HT,CFD}}$ presented in Table 3 for the Cai mechanism is obtained by performing a 3-D LES reacting spray combustion simulation using the numerical setup presented in the current work. On the other hand, the $\text{IDT}_{\text{HT,CFD}}$ for the Polimi and Stanford mechanisms shown in Table 3 are obtained from the LES results performed independently and separately by Wehrfritz et al. [31] under similar Spray A conditions at T_{amb} of 900 K. Despite obtaining the $\text{IDT}_{\text{HT,CFD}}$ from a different numerical setup [31] than the present work, the $\text{IDT}_{\text{HT,CTS}}$ computed using the proposed method are still comparable with the $\text{IDT}_{\text{HT,CFD}}$ values therein. The relative difference for the Polimi and Stanford mechanisms are within 12%. This further demonstrates the feasibility of the proposed prediction method in predicting IDT of reacting spray combustion using different chemical mechanisms.

4. Conclusion

The Coupled Time Scale (CTS) method is proposed to estimate the high-temperature ignition delay time (IDT) of liquid spray combustion. The method is applied to *n*-dodecane spray under the ECN Spray A and Spray D conditions at ambient temperature (T_{amb}) of 800 K, 900 K, and 1000 K, where their ignitions are shown to initiate at mixtures close to the most reactive mixture fraction (Z_{mr}). The method requires the probability density functions of mixture fraction (Z) computed from 3-D LES inert spray cases, as well as the Z_{mr} and most reactive IDT (IDT_{mr})

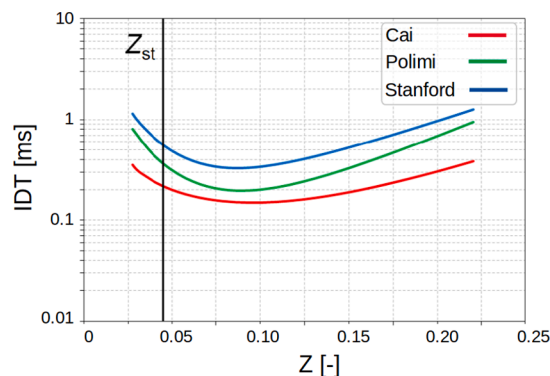


Fig. 8. Ignition delay time (IDT) of homogeneous mixtures as a function of mixture fraction (Z) for Spray A at $T_{\text{amb}} = 900\text{K}$ from different mechanisms.

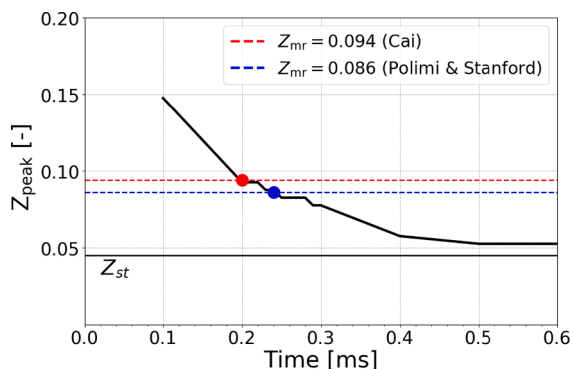


Fig. 9. Temporal evolution of mixture fraction at peak PDF (Z_{peak}) for Spray A at $T_{\text{amb}} = 900$ K. Horizontal dashed-lines represent most reactive mixture fraction (Z_{mr}) for different mechanisms. Symbols (•) indicate t_{mr} .

Table 3
IDTs and relative differences for different chemical mechanisms.

Mechanisms	IDT _{HT,CTS} [ms]	IDT _{HT,CFD} [ms]	Relative difference %
Cai	0.350	0.333	5.1
Polimi	0.438	0.390 [31]	11.4
Stanford	0.570	0.530 [31]	8.6

obtained from the 0-D homogeneous reactor simulations. The fidelity of the proposed CTS method is verified by comparing the predicted IDT ($IDT_{\text{HT,CTS}}$) against the measured IDT and CFD simulated IDT. The relative difference of $IDT_{\text{HT,CTS}}$ to measured IDT are less than 24%. Meanwhile, the relative differences between the $IDT_{\text{HT,CTS}}$ and the computed IDT from CFD calculation are within 33% across different T_{amb} , D_{noz} and chemical mechanisms. It is noteworthy that scalar dissipation rate is not considered in this method, which is likely the cause for the larger discrepancy observed at low T_{amb} . Nevertheless, the proposed method is shown to be capable of estimating the high-temperature IDT of reacting spray combustion under the tested conditions.

Declaration of Competing Interest

The authors declare that they have no known competing financial interests or personal relationships that could have appeared to influence the work reported in this paper.

Acknowledgement

The authors gratefully acknowledge the financial support from the Independent Research Fund Denmark (DFF) and MAN Energy Solutions under the Grant No. 8022-00143B. The computation was performed using Niflheim cluster at Technical University of Denmark (DTU).

References

- [1] Engine combustion network. <https://ecn.sandia.gov/>.
- [2] Shen H-PS, Steinberg J, Vanderover J, Oehlschlaeger MA. A shock tube study of the ignition of n-heptane, n-decane, n-dodecane, and n-tetradecane at elevated pressures. *Energy Fuels* 2009;23(5):2482–9.
- [3] Desantes JM, López JJ, García-Oliver JM, López-Pintor D. Experimental validation and analysis of seven different chemical kinetic mechanisms for n-dodecane using a rapid compression-expansion machine. *Combust Flame* 2017;182:76–89.
- [4] Pei Y, Hawkes ER, Kook S. A comprehensive study of effects of mixing and chemical kinetic models on predictions of n-heptane jet ignitions with the PDF method. *Flow Turbulence Combust* 2013;91(2):249–80.
- [5] Pang KM, Jangi M, Bai X-S, Schramm J, Walther JH, Glarborg P. Effects of ambient pressure on ignition and flame characteristics in diesel spray combustion. *Fuel* 2019;237:676–85.
- [6] Mastorakos E, Baritaud T, Poinso T. Numerical simulations of autoignition in turbulent mixing flows. *Combust Flame* 1997;109(1–2):198–223.
- [7] Mastorakos E. Ignition of turbulent non-premixed flames. *Prog Energy Combust Sci* 2009;35(1):57–97.
- [8] Schroll P, Wandel AP, Cant RS, Mastorakos E. Direct numerical simulations of autoignition in turbulent two-phase flows. *Proc Combust Inst* 2009;32(2):2275–82.
- [9] Borghesi G, Mastorakos E, Cant RS. Complex chemistry DNS of n-heptane spray autoignition at high pressure and intermediate temperature conditions. *Combust Flame* 2013;160(7):1254–75.
- [10] Zhou T, Zhao M, Zhu M, Ye T, Liu M. Three-dimensional direct numerical simulation of n-dodecane spray autoignition with complex chemistry. *Energy Fuels* 2018;32(9):9838–49.
- [11] Borghesi G, Krisman A, Lu T, Chen JH. Direct numerical simulation of a temporally evolving air/n-dodecane jet at low-temperature diesel-relevant conditions. *Combust Flame* 2018;195:183–202.
- [12] Krisman A, Hawkes ER, Talei M, Bhagatwala A, Chen JH. A direct numerical simulation of cool-flame affected autoignition in diesel engine-relevant conditions. *Proc Combust Inst* 2017;36(3):3567–75.
- [13] Pei Y, Som S, Pomraning E, Senecal PK, Skeen SA, Manin J, Pickett LM. Large eddy simulation of a reacting spray flame with multiple realizations under compression ignition engine conditions. *Combust Flame* 2015;162(12):4442–55.
- [14] Dahms RN, Paczk GA, Skeen SA, Pickett LM. Understanding the ignition mechanism of high-pressure spray flames. *Proc Combust Inst* 2017;36(2):2615–23.
- [15] Westlye F. Experimental Study of Liquid Fuel Spray Combustion (PhD Dissertation). Technical University of Denmark (DTU) 2016.
- [16] Kim W-W, Menon S. A new dynamic one-equation subgrid-scale model for large eddy simulations. 33rd Aerospace Sciences Meeting and Exhibit 1995:356.
- [17] Reitz RD, Diwakar R. Structure of high-pressure fuel sprays. *SAE Trans* 1987: 492–509.
- [18] Yao T, Pei Y, Zhong B-J, Som S, Lu T, Luo KH. A compact skeletal mechanism for n-dodecane with optimized semi-global low-temperature chemistry for diesel engine simulations. *Fuel* 2017;191:339–49.
- [19] Ma PC, Wu H, Jaravel T, Bravo L, Ihme M. Large-eddy simulations of transcritical injection and auto-ignition using diffuse-interface method and finite-rate chemistry. *Proc Combust Inst* 2019;37(3):3303–10.
- [20] Kahila H, Wehrfritz A, Kaario O, Vuorinen V. Large-eddy simulation of dual-fuel ignition: Diesel spray injection into a lean methane-air mixture. *Combust Flame* 2019;199:131–51.
- [21] Chomiak J, Karlsson A. Flame liftoff in diesel sprays. In: *Symp. (Int.) Combust.*, vol. 26. Elsevier; 1996. p. 2557–64.
- [22] Jangi M, Yu R, Bai X-S. Development of chemistry coordinate mapping approach for turbulent partially premixed combustion. *Flow Turbulence Combust* 2013; 90(2):285–99.
- [23] Pang KM, Jangi M, Bai X-S, Schramm J, Walther JH. Modelling of diesel spray flames under engine-like conditions using an accelerated eulerian stochastic field method. *Combust. Flame* 2018;193:363–83.
- [24] Gimeno J, Bracho G, Martí-Aldaraví P, Peraza JE. Experimental study of the injection conditions influence on n-dodecane and diesel sprays with two ECN single-hole nozzles. Part I: Inert atmosphere. *Energy Convers Manage* 2016;126: 1146–56.
- [25] Pastor JV, García-Oliver JM, García A, López AM. An experimental investigation on spray mixing and combustion characteristics for Spray C/D nozzles in a constant pressure vessel, *SAE Technical Paper* 2018-01-1783, 2018.
- [26] Desantes JM, García-Oliver JM, Novella R, Pachano L. A numerical study of the effect of nozzle diameter on diesel combustion ignition and flame stabilization. *Int J Engine Res.*
- [27] Kundu P, Ameen MM, Som S. Importance of turbulence-chemistry interactions at low temperature engine conditions. *Combust Flame* 2017;183:283–98.
- [28] Davidovic M, Falkenstein T, Bode M, Cai L, Kang S, Hinrichs J, Pitsch H. Les of n-dodecane spray combustion using a multiple representative interactive flamelets model. *Oil Gas Sci Technol-Revue d'IFP Energies Nouvelles* 2017;72(5):29.
- [29] Ranzi E, Frassoldati A, Stagni A, Pelucchi M, Cuoci A, Faravelli T. Reduced kinetic schemes of complex reaction systems: fossil and biomass-derived transportation fuels. *Int J Chem Kinet* 2014;46(9):512–42.
- [30] Narayanaswamy K, Pepiot P, Pitsch H. A chemical mechanism for low to high temperature oxidation of n-dodecane as a component of transportation fuel surrogates. *Combust Flame* 2014;161(4):866–84.
- [31] Wehrfritz A, Kaario O, Vuorinen V, Somers B. Large eddy simulation of n-dodecane spray flames using Flamelet Generated Manifolds. *Combust Flame* 2016;167: 113–31.